

See discussions, stats, and author profiles for this publication at: <https://www.researchgate.net/publication/332259889>

Designing a New Dynamic Mechanical Analysis (DMA) System for Testing Viscoelastic Materials at High Frequencies

Article in *Modelling and Simulation in Engineering* · April 2019

DOI: 10.1155/2019/7026267

CITATIONS

0

READS

48

5 authors, including:



[Roja Esmaeeli](#)

University of Akron

15 PUBLICATIONS 39 CITATIONS

[SEE PROFILE](#)



[Haniph Aliniagerdroudbari](#)

University of Akron

14 PUBLICATIONS 39 CITATIONS

[SEE PROFILE](#)



[Siamak Farhad](#)

University of Akron

58 PUBLICATIONS 681 CITATIONS

[SEE PROFILE](#)

Some of the authors of this publication are also working on these related projects:



Project Proton Exchange Membrane Fuel Cells [View project](#)



Project ENERGY HARVESTING SYSTEM FOR TIRE MONITORING APPLICATIONS [View project](#)

Research Article

Designing a New Dynamic Mechanical Analysis (DMA) System for Testing Viscoelastic Materials at High Frequencies

Roja Esmaeeli , Haniph Aliniagerdroudbari, Seyed Reza Hashemi, Chiran JBR, and Siamak Farhad 

Advanced Energy & Sensor Lab, The University of Akron, Akron, Ohio, USA

Correspondence should be addressed to Siamak Farhad; sfarhad@uakron.edu

Received 13 August 2018; Revised 20 November 2018; Accepted 10 February 2019; Published 25 March 2019

Academic Editor: Gaetano Sequenzia

Copyright © 2019 Roja Esmaeeli et al. This is an open access article distributed under the Creative Commons Attribution License, which permits unrestricted use, distribution, and reproduction in any medium, provided the original work is properly cited.

The aim of this study is to design a new dynamic mechanical analysis (DMA) measurement system that can operate for shear tests at frequencies as high as 10 kHz with strain amplitudes sufficient for viscoelastic materials operating in high-frequency deformation applications, such as tire rubbers. The available DMA systems in market cannot effectively operate for accurate and direct measurement of viscoelastic material properties for applications dealing with high-frequency deformation of materials. Due to this, the available DMA systems are used for indirect measurements at low frequencies and low temperatures, followed by using time-temperature superposition principle to predict the properties at high frequencies. The goal of this study is to make the range of the test broad enough to eliminate the use of the time-temperature superposition principle in the determination of properties of viscoelastic materials. Direct measurement of viscoelastic material properties and increasing the accuracy of results are the main motivations to design a new DMA system. For this purpose, the state-of-the-art technologies to achieve high frequencies and strain amplitudes as well as instrumentation and control of the system are studied. The design process is presented in this paper.

1. Introduction

Unlike elastic and viscous behavior, some materials, such as rubber, resemble a viscoelastic characteristic upon deformation. This behavior is similar neither to what is seen in a purely elastic material where the phase difference between the stress and strain waves is zero degrees nor to the response of a purely viscous material where the phase difference between the stress and strain waves is 90 degrees. In this case, the phase difference falls somewhere between these two extremes [1]. If a phase difference closer to zero degree is reported, the elastic behavior is more likely to be seen, and consequently, the storage modulus is greater than its loss modulus. On the contrary, when the phase difference is closer to the other end of this spectrum, viscous characteristic will be more dominant than its elastic characteristics resulting in a greater loss modulus compared to the storage modulus. In a viscoelastic material, the material temperature and the frequency of strain and stress waves play important roles in defining the phase difference between these two

waves. In a tire, the road contact area with tire tread determines the frequencies of the rubber expansion-contraction when the tire rotates on the road. In addition to the rubber chemical composition, the properties of phase difference and the storage/loss modulus of the rubber treads depend on the road texture profile wavelengths. There are different configurations of road texture profiles that determine the rubber tread expansion-contraction frequencies and the rubber dry and wet tractions. Nowadays, the attention to the vehicle safety is increased specially with the newly developed autonomous vehicles [2, 3]. Casualty and fatality in car accidents highly depend on road condition. Statistically, probability of accidents is two to three times more when roads are wet [4–8]. Therefore, investigations to study the rubber tread properties at frequencies corresponding to the rubber wet friction are highly supported. Researchers try to predict the rubber compound wet traction, and it is reported that rubber viscoelastic properties should be measured at the range of frequencies of 1 kHz to 1 MHz [9–12].

Dynamic mechanical analysis (DMA) is a promising approach to analyze the data extracted from applying a stress or strain to a viscoelastic material to measure the phase angle and deformation data from which the damping factor, $\tan \delta$, is obtained and the complex modulus and viscosity data are calculated thereafter. In different DMAs, there are two approaches that are applied for measurement: (a) forced vibration, where the vibration is applied at a set frequency below to the natural frequency of the specimen, and (b) free resonance, where the material is perturbed and allowed to exhibit free resonance decay. The approach based on forced vibration is more utilized and commercialized more frequently. DMAs and their applications have been described in several publications [1, 13–18]. Especially, readers are referred to the papers published by Nolle [19] and te Nijenhuis [20]. ASTM standards are also suitable sources to use DMA systems [21]. Mostly, the maximum frequency of commercial conventional DMAs is limited to 1000 Hz for shear tests. In order to overcome this limitation, researchers in tire industry employ the time-temperature superposition principle. In fact, researchers decrease the temperature of rubber and perform the test at low frequencies and then use master curves or the Williams–Landel–Ferry (WLF) equation [22] to predict the rubber properties at high frequencies. Although the time and temperature dependency of properties is a characteristic of viscoelastic materials [23, 24], the WLF equation constants cannot be easily obtained for different rubbers [15]. The equation constants of the WLF equation or master curves that tire manufacturers usually use are obtained for certain rubber compounds. Thus, using this method for new rubber compounds may not necessarily lead to an accurate determination of the rubber properties at high frequency.

For improved prediction of the rubber properties at high frequencies, especially for newly developed rubber compounds, the rubber viscoelastic properties should be measured accurately and directly at a desired frequency rather than using the time-temperature superposition principle. There are a few cases of high-frequency testing (up to 5 kHz) of viscoelastic materials available in the literature, but only for tension compression tests [25–28]. At present, the only commercial DMA for high-frequency testing is METRAVIB VHF104 [29] and works based on bringing the specimen to the resonance and recording transmissibility data. An existing limitation for this test is lack of practical know-how to statically preload the specimen further than a limit for desired preload amount. The other limitation is that in order to run the shear test with VHF104, setting up the raw material inside the sheared gap and thus curing the material while being held in a specimen holder is inevitable prior to testing; hence, there is no chance of testing the aged material with this setup. The third limitation of working with METRAVIB VHF104 is its inability to monitor and control the strain range. In other words, the test setup uses stress-driven process, and the amount strain is dependent on the material characteristics, mostly stiffness and geometry. This makes the strain amount difficult to keep in check. Furthermore, there are no available publications on the METRAVIB VHF104 shear test. Due to all the difficulties the

current DMAs have, the goal of this study is to design a new DMA test system that can operate at frequencies as high as 10 kHz in forced vibration mode for shear test. This test system can be generally used for the determination of properties of a broad range of viscoelastic materials for applications where the material experiences high-frequency deformations. Of course, the application of such a test system for tire industry is the direct measurement of rubber mechanical properties without using the WLF equation for predicting wet traction.

2. Design

Designing a new DMA system, operating at high frequencies, requires establishing an algorithm to calculate the properties of viscoelastic materials from basic measurements, choosing appropriate actuator and its amplifier, designing a closed-loop control system to adjust the actuator displacement at the desired value, choosing a force sensor, choosing a multichannel data acquisition board with high resolution and very high sampling rates, calculation of drag force against the movement of actuator and clamp, calculation of the heat build-up in the rubber specimen during the test, designing a clamp holding the rubber specimen, natural resonance and stress analyses of the clamp, etc. The focus of this paper is only on some of the design aspects of the new DMA system. It is noted that this new DMA is designed for rubber to go through simple shear.

In this section, first, the algorithm of calculations for the determination of properties of viscoelastic materials from basic measurements is presented. Then, determination of the optimum rubber specimen size for the test is discussed, followed by calculation of the drag force against the clamp movement and heat built-up in the specimen during the test. Then, the piezoelectric actuator and its amplifier required for the new DMA system are introduced. Finally, the design of the clamp is illustrated.

2.1. Algorithm of Calculations in DMA System. The algorithm starts from analyzing the stress, σ , resulted from the applied sinusoidal displacement, to the viscoelastic material specimen at the given frequency. The stress is obtained from the force sensor and the surface area of the specimen. The displacement is adjusted by the actuator controller. The frequency and the sine wave are generated by a function generator connected to the actuator amplifier. The phase angle, δ , can be calculated from the time lag between the stress and strain sine waves, leading to computation of damping factor, $\tan \delta$, complex shear modulus, G^* , loss modulus, G'' , and storage modulus, G' , as shown in Figure 1.

2.2. Actuator. The actuator considered for the new DMA system is a piezoelectric actuator. One of the concerns when using these actuators is the push and pull forces required for the system operation. Basically, piezoelectric actuators can provide push force but they are not strong enough to provide the same pull force. Thus, it is necessary to calculate the required force for the piezoelectric actuator

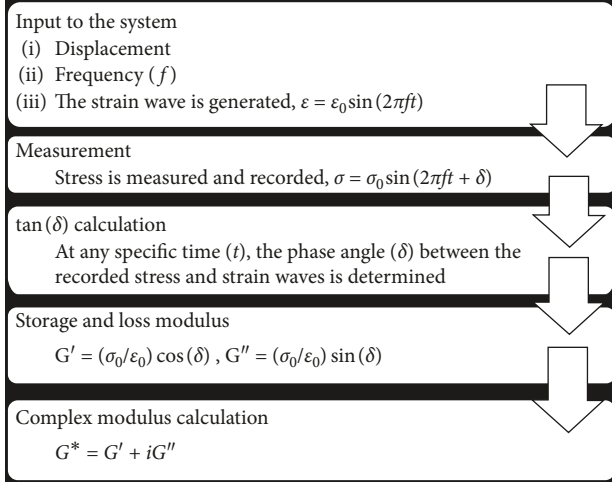


FIGURE 1: Algorithm of calculating mechanical properties of viscoelastic materials in DMA systems.

in different frequencies and amplitudes of the DMA system operation to choose an appropriate piezoelectric actuator. For this purpose, first, the dependency of complex shear modulus on frequency is tested based on the typical data reported in [30]. Then, using the shear modulus, the maximum power, P , required to move two specimens at the upper limit frequency of the new DMA system, which is 10 kHz, and the strain amplitude of 0.05% is calculated from the following equation:

$$P = 8f_0\epsilon_0^2hG^*A, \quad (1)$$

where h is the thickness of the specimen, G^* is the complex shear modulus, and A is the surface area of the specimen. It is noted that this power is needed for oscillation of two specimens sandwiched between the moving clamp and two stationary metal parts as shown in Figure 2.

In the second step, $P_{10,0.05}$ (maximum power at frequency of 10 kHz and strain amplitude of 0.05%) is considered a constant input to calculate the maximum strain amplitude of the specimen and the needed force at every frequency below 10 kHz from Equations (2) and (3), respectively. The results of these calculations are presented in Section 3.

$$\epsilon = \left(\frac{P_{10,0.05}}{8fhG^*A} \right)^{0.5}, \quad (2)$$

$$F = 2\epsilon G^*A. \quad (3)$$

After determination of the maximum force required to run the new DMA, a piezoelectric actuator with specifications listed in Table 1 is chosen. In addition, the piezoelectric amplifier working diagram is used to calculate the actuator displacement for each frequency.

2.3. Size of Specimen. In the process of choosing the specimen size, three factors have to be taken into consideration. The first factor is the effect of the size on the required force, power, and displacement of the actuator. The second factor

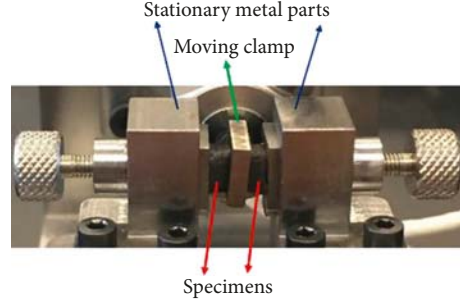


FIGURE 2: Two specimens sandwiched between the moving clamp and two stationary metal parts.

TABLE 1: Specifications of the chosen stacked preloaded piezoelectric actuator.

Item	Value	Unit
Closed-loop travel	15	μm
Closed-loop resolution	0.3	nm
Push/pull force	800/300	N
Electrical capacitance	1.8 ± 20%	μF
Unloaded resonant frequency (f_0)	18 ± 20%	kHz
Standard operating temperature range	-20 to +80	°C
Weight without cables	31 ± 5%	g
Length, L	37 ± 0.3	mm

is to avoid the shear elastic wave, which might have troublesome effects on the results of the measurements. The third factor is the simplicity in preparation of the specimen for the DMA users.

While shear stress is exerted to the specimen, the top surface of the specimen starts oscillating, which will be propagated into the rubber as a transverse elastic wave. This incipient propagation of shear elastic wave shall be treated in a way to avoid affecting the test results, which means the specimen thickness must be much smaller than the wavelength of the shear elastic wave [31] or the value of $G^*/h^2f^2\rho$ of the specimen should be much larger than unity [15] (G^* is shear modulus, h is specimen thickness, f is the frequency of the oscillation, and ρ is the target material density).

The speed of shear elastic wave propagations is calculated from the following equation:

$$v = \sqrt{\frac{G^*}{\rho}}. \quad (4)$$

A method to avoid the shear deformation is to limit the ratio of thickness to length of the specimen to amounts less than 1/4 [32] or 1/3 [33]. In this study, the ratio of thickness to length of the specimen is taken 1/3.

2.4. Air Drag against the Clamp Movement. The drag or resistance force of specimen moving object in a fluid can be quantified as

$$F_D = \frac{1}{2}C_d\rho A_a V^2, \quad (5)$$

where V is the velocity, A_a is the area of the rubber specimen and clamp facing the air movement, and ρ is the fluid density. The drag coefficient, C_d , is dependent on various factors including the object speed and direction, object position, object geometry, fluid density, viscosity, etc. In this study, C_d is considered to be 1.28 [34].

2.5. Heat Generation in the Specimen. As shown in Figure 2, two specimen blocks are located between two stationary metal parts and the clamp. These two metal parts and the clamp are considered as ideal heat sinks for the specimens. The maximum temperature reached in the specimen is determined using the finite element analysis (FEA) method. Equation (6) represents the heat generation in the viscoelastic materials as a function of frequency and strain amplitude. For simulation of heat transfer in the specimen, the COMSOL Multiphysics software is used. Readers may refer to [35] to find more details on the heat generation model.

$$\dot{Q} = 4AhG'' f \varepsilon_0^2 \sin^2(2\pi ft). \quad (6)$$

2.6. Clamp Design. The conventional procedure of using a single specimen shear test can be implemented; however, this may be in need of a truly rigid clamp, which means for applying the shear force, it has to consider a rigid clamp that can provide attachments between the specimen and the clamp during the test. Geometry of the specimen must be controlled cautiously so as to make modulus data thoroughly meaningful [17]. In addition, since the use of a single specimen could be problematic in axial loading [36], it is practically more convenient to use a double-sandwich setup, which conducts the test on a pair of specimens together. Further information on this shear test can be found in the ASTM D5992 [37]. Due to thermal expansion of the fixture which will boost fluctuations in clamping force values and apply different value of forces to specimen surfaces in contact by the clamp, the double-sandwich setup can be hard for testing under conditions of broad temperature ranges [17]. The quadruple shear test is the other method that uses four replicate specimens and avoids the need for rigid restraining fixtures [36].

For carrying out the test at high frequencies with the piezoelectric actuator, the applied force to the specimen should be diminished in a way that the piezoelectric actuator can provide the required force. Therefore, among the mentioned approaches, the double-sandwich shear test is used. In addition, in the conventional DMAs, the double-sandwich clamp is placed in the temperature chamber to apply broad temperature ranges to the rubber, and the rubber properties is calculated with the use of WLF equation [22] as described before. Usually, the clamp is made of metal, and thermal expansion of the metal causes some difficulties to hold the rubber specimen inside the clamp. Due to the fact that the designed clamp works at room temperature and directly measures the rubber dynamic properties, thermal expansion of the clamp would not be a concern. The clamp is designed in SOLIDWORKS, and a detailed design is

presented by the authors in [38]. The FEA on natural resonance and stress analyses are conducted in the COMSOL Multiphysics software in order to find the natural frequency of the clamp and ensure that it can withstand high frequencies.

3. Results and Discussion

3.1. Dependency of Shear Modulus to Frequency. Most properties of viscoelastic materials are dependent on time (frequency). In Figure 3, this reliance is plotted for the shear modulus based on data presented in [30].

3.2. Size of Specimen, Displacement, and Force. The required specimen displacement (solid line) and the ability of the chosen piezoelectric actuator displacement (dash-dot line) at different frequencies are shown in Figure 4. It is obvious that at high frequencies, the needed displacement for the 3 mm and 2.5 mm thickness specimens is more than the displacement that the piezoelectric actuator can provide, thus these two specimen sizes are not applicable. In addition, in testing frequency of 100 Hz, all the specimen sizes except the one with 1 mm thickness are not useful due to their higher demand of displacement which the piezoelectric actuator is not capable of providing. For the frequency of 250 Hz, only 3 mm and 2.5 mm thickness specimens are not fitted in the piezoelectric actuator displacement range. Overall, the chosen piezoelectric actuator can provide the required displacement of the specimen in the range of the frequencies of 250 Hz and 10 kHz if the thickness of the specimen is less than 2.5 mm.

The constant power curve of the frequency-amplitude of the DMA has been calculated based on the power required to provide 0.05% strain at the frequency of 10 kHz. This curve (dash-dot line) is shown in Figure 5. It is desired that DMA operates at any point underneath this curve. From the other side, the required force for the piezoelectric actuator for several specimen thicknesses is calculated at different frequencies and shown in Figure 5 (solid lines). In frequency of 100 Hz for 3 mm and 2.5 mm specimen thickness, the piezoelectric actuator has to provide 61.0 N and 43.5 N, respectively. If the thickness of specimen decreases, the force required to run the test decreases.

We calculated that the wavelength of the elastic wave for 10 kHz, 1 kHz, and 100 Hz would be almost 41 mm, 129 mm, and 1291 mm, respectively. In addition, the ratio of $G^*/h^2 f^2 \rho$ for 1, 1.5, 2, 2.5, and 3 mm specimen thicknesses, as presented in Table 2, is much more than unity. Therefore, the measurement results in the new DMA will not be influenced by the elastic wave discussed earlier, and the inertial forces will be small for all the studied specimen sizes.

The air drag force against the clamp movement at different frequencies, specimen strains, and specimen thicknesses is plotted in Figure 6. It is presumed that at high frequencies, less strain is needed, and as the frequency decreases, the strain increases. This is in accordance with the

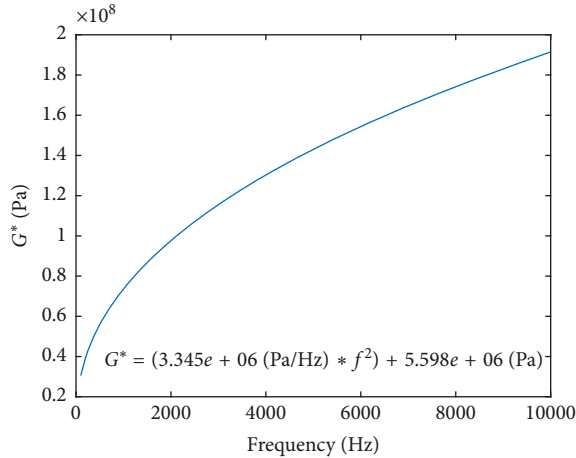


FIGURE 3: The relation between shear modulus and frequency of a typical viscoelastic material.

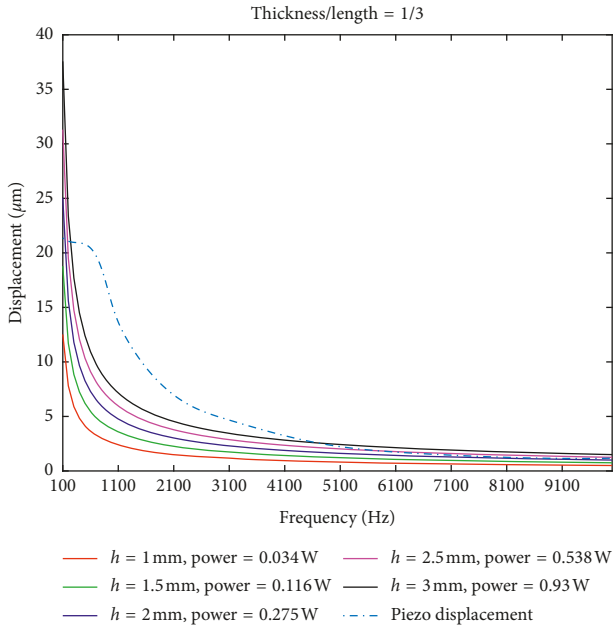


FIGURE 4: The relation between the required displacement and the ability of the piezoelectric actuator displacement at different frequencies.

constant power criterion explained before. It is obvious that by increasing the specimen thickness, frequency, or strain, the force will increase accordingly. The results show that the maximum drag force in the worst scenario will be $5.4e-7$ N, which is negligible compared to the force required to accelerate the clamp and specimen. Consequently, there will be no need to place the test setup in the vacuum chamber.

Overall, based on the results in Figures 4–6, the thickness of specimens more than 2.5 mm is not possible for this design because of the chosen piezoelectric limitations. Any thicknesses between 1 mm and 2 mm are suggested for the thickness of the specimen. However, for simplicity of the sample preparation by the DMA users, the 2 mm thickness is finally chosen. Thus, the specimen size would be $2 \times 6 \times 6$ mm³.

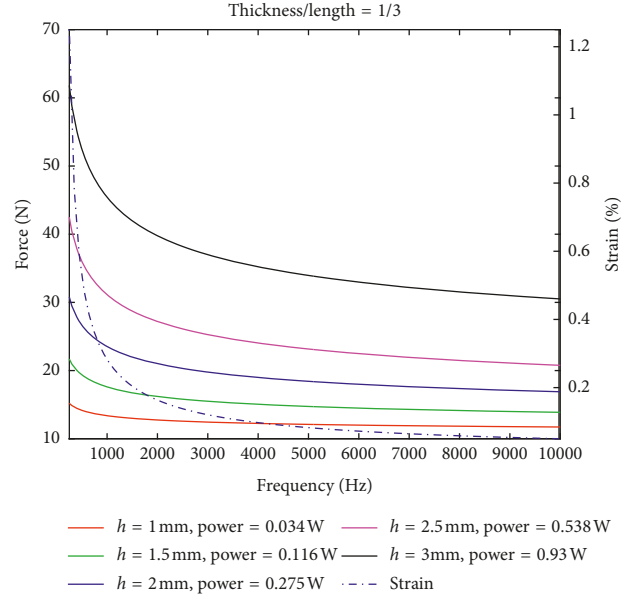


FIGURE 5: The force needed to oscillate two specimens.

TABLE 2: The $G^*/h^2 f^2 \rho$ ratio for different rubber specimen sizes and frequencies.

Frequency (Hz)	Specimen thickness (mm)	$G^*/h^2 f^2 \rho$
10,000	1.0	1,667
1,000	1.0	16,667
100	1.0	1,666,667
10,000	1.5	741
1,000	1.5	7,407
100	1.5	740,741
10,000	2.0	417
1,000	2.0	4,167
100	2.0	416,667
10,000	2.5	267
1,000	2.5	2,667
100	2.5	266,667
10,000	3.0	185
1,000	3.0	1,852
100	3.0	185,185

3.3. Specimen Temperature Increase due to the Build-Up Heat during Test. The maximum temperature increase in the rubber specimen due to the heat build-up during the test is determined using FEA analysis. Results are labeled in Table 3. The maximum temperature increase for the conventional DMAs is also compared with the new DMA in this table. The conventional DMA specimen size is chosen from [35]. The conventional DMAs usually run the test at high strain and low frequencies, so it is assumed that the conventional DMA test is run for the 30% strain at a frequency of 1Hz. The results indicate the maximum temperature increase in the specimen for the conventional DMA test will be 18.9°C; however, for the new test setup, it would not be more than 3.8°C. The specimen temperature increase during different conventional DMA tests is studied in [35]. It is shown that there is a huge temperature increase happening inside the specimen during the conventional DMA tests, which may affect the DMA tests results.

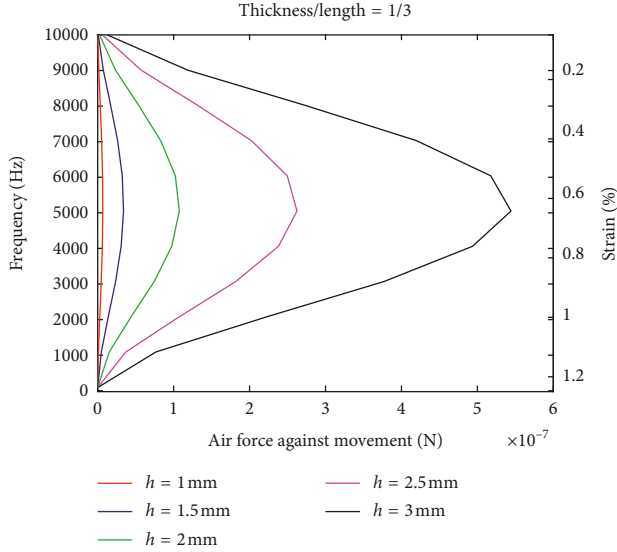


FIGURE 6: The drag force against the clamp movement.

TABLE 3: The maximum temperature increase in the rubber specimen due to the heat build-up during the test.

DMA test device	Frequency (Hz)	Strain (%)	Specimen dimension (mm ³)	Maximum temperature increase (°C)
Conventional	1	30	5 × 16 × 40	18.9
New test setup	1000	0.25	2 × 6 × 6	3.8
	5000	0.08		1.9
	10000	0.05		1.5

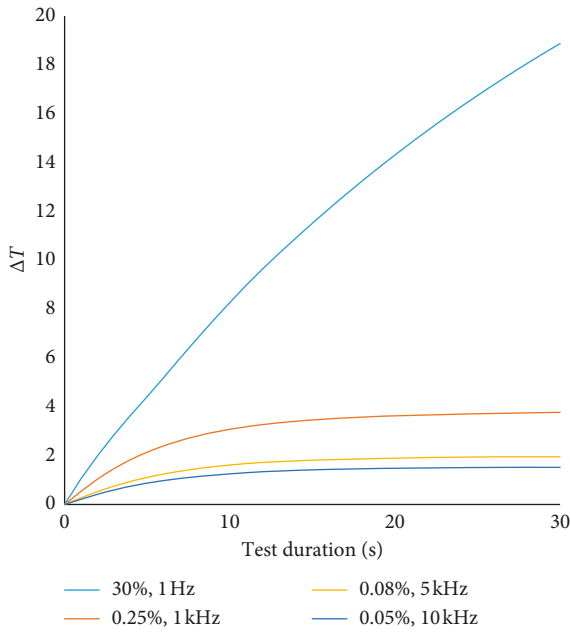


FIGURE 7: The increase of the maximum temperature of the rubber specimen due to the heat build-up during the test.

3.4. Clamp Design and Test Setup. Figure 8 illustrates the vertical and horizontal designs of the test setup. In Figure 8(b), the new DMA test system components are defined. The clamp material would be steel AISI 4340. Two different designs were considered to find out which one has

higher natural frequency to be used in a high-frequency DMA system. The results of the Eigen frequency analysis with the COMSOL Multiphysics software show that the horizontal design with the first natural frequency of 20 kHz can endure the test conditions.

In both designs, the piezoelectric actuator is attached to a force sensor for measuring the force, and this force sensor will transfer the load to the rod that provides movement in the two rubber specimens. Hence, the piezoelectric actuator needs to provide force for movement of all the design. By considering the steel material, the force sensor weight is 14 g, and the designed connection rod is 10 g. For this case, the total force is obtained and demonstrated in Figure 9. It is obvious that for the specimen thickness of 2 mm, the maximum force required is about 160 N, which is not more than the piezoelectric actuator capability as seen in Table 1. The maximum push and pull forces of the chosen stacked preloaded piezoelectric actuator are 800 N and 300 N, respectively, as referenced in Table 1; however, in the new DMA system, there is a need for push and pull forces same as each other; thus, the maximum force capability of piezo actuator is 300 N. In addition, by increasing the frequency and decreasing the strain, as it is shown in Figure 5, the needed force for providing movement in specimen is decreased; however, increasing the frequency results in increasing the acceleration; thus, the total needed force as it is obvious in Figure 9 is increased.

The working window of the new DMA system is illustrated in Figure 10. As shown, the starting frequency is 250 Hz with 0.67% strain and 14.1 μ m displacement of the

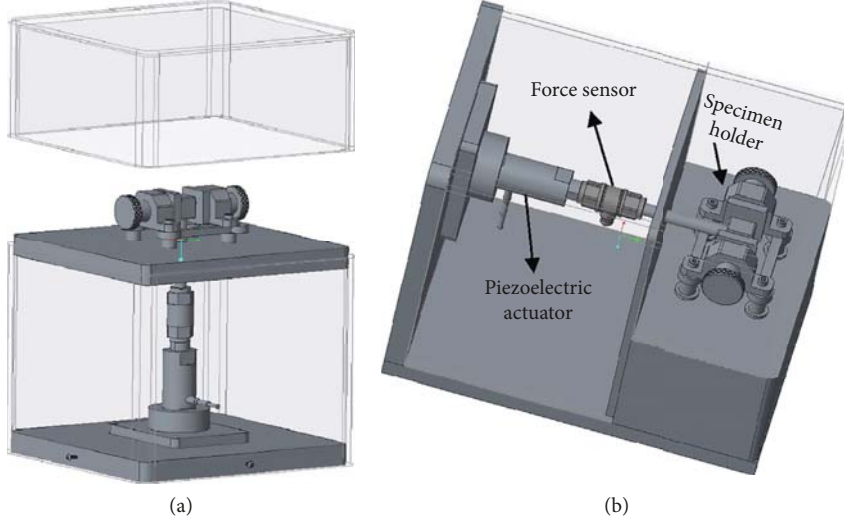


FIGURE 8: Clamp design: (a) vertical and (b) horizontal.

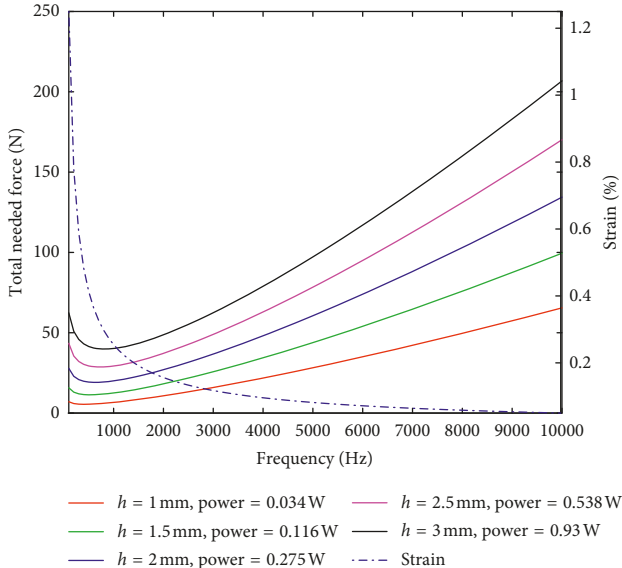


FIGURE 9: Total force needed at different frequencies.

piezoelectric actuator. The ending frequency is 10 kHz with 0.05% strain and $1.5 \mu\text{m}$ displacement of the piezoelectric actuator. Any point underneath this curve is considered the operating point of the new DMA system.

Figure 11 shows the piezoelectric actuator displacement capability and the needed displacement for running the test in the range of 250 Hz to 10 kHz.

4. Conclusion

The process of designing a new DMA test system for operating at high frequencies was described in this paper. This new DMA system can be used for measurement of mechanical properties of viscoelastic materials for applications where high-frequency deformation of these materials is required. One of the applications of this new DMA system is for testing the rubber treads for tires. Using this

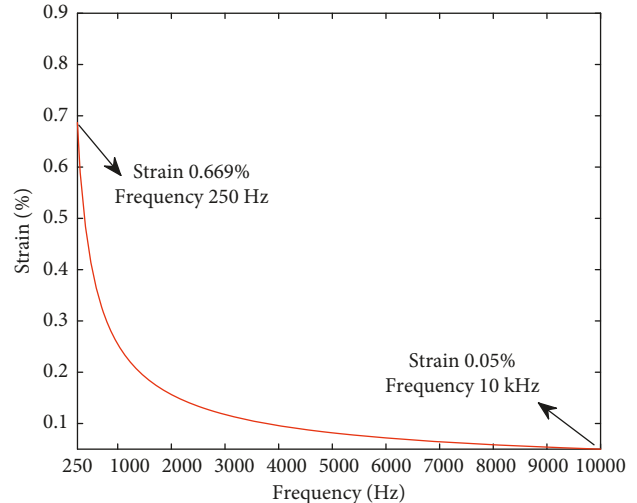


FIGURE 10: The working window of the new DMA system.

high-frequency system, one can conduct a direct measurement for a new rubber compound rather than using the time-temperature superposition principle. The system setup for the new DMA includes a high-load piezoelectric actuator, a low-weight force sensor, and a new designed test clamp. It is predicted that the new DMA system can operate in a broad frequency range, from 250 Hz with maximum strain amplitude of 0.67% to 10 kHz with the maximum strain amplitude of 0.05%. During the design process, the force needed for making oscillation in the viscoelastic material specimen and the displacement during the test for four sizes of specimen thicknesses were compared. According to the piezoelectric actuator capabilities for providing force and displacement in high frequencies, the 2 mm thickness specimen was chosen. The specimen size of $2 \text{ mm} \times 6 \text{ mm} \times 6 \text{ mm}$ was finally chosen. Horizontal and vertical clamps were designed, and the Eigen frequency analysis with the COMSOL Multiphysics software shows that the horizontal design with the first natural frequency of

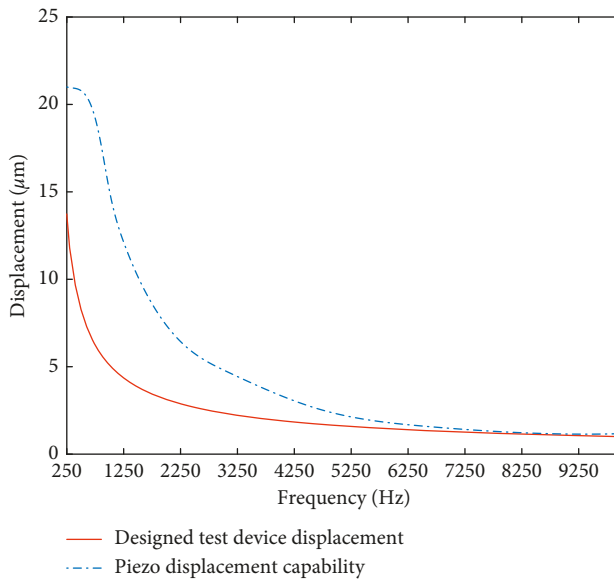


FIGURE 11: The piezoelectric actuator displacement capability and the needed displacement for the new DMA system.

20 kHz is the best clamp design. The effect of elastic wave propagation was also examined to make sure its effect will not interfere with the results of the DMA system. The maximum temperature increase in the rubber specimen due to the heat build-up during the test was also obtained. This temperature will be less than 3.8°C in the worst scenario, which is acceptable for a DMA system.

Nomenclature

σ :	Stress
σ_0 :	Initial stress
ε :	Strain
ε_0 :	Initial strain
δ :	Phase angle
ρ :	Density
A :	Surface area
C_d :	Drag coefficient
f :	Frequency
f_0 :	Initial frequency
F :	Force
G' :	Storage shear modulus
G'' :	Loss shear modulus
G^* :	Complex shear modulus
h :	Specimen thickness
P :	Power
Q :	Rate of heat generation
$\tan \delta$:	Damping factor
t :	Time
T_g :	Glass temperature
v :	Velocity.

Data Availability

The data used to support the findings of this study are included within the article.

Conflicts of Interest

The authors declare that they have no conflicts of interest.

Acknowledgments

The authors appreciate the financial supports of CenTiRe, NSF, and University of Akron. Also special thanks are due to mentors who have been actively involved and helpful in this survey. This project has been supported by NSF-I/UCRC, Center for Tire Research (CenTiRe).

References

- [1] M. Sepe, *Dynamic Mechanical Analysis for Plastics Engineering*, William Andrew, Norwich, CT, USA, 1998.
- [2] R. Esmaeli, H. Aliniagerdroudbari, S. R. Hashemi et al., "A rainbow piezoelectric energy harvesting system for intelligent tires monitoring applications," *Journal of Energy Resources Technology*, vol. 141, no. 6, article 062007, 2018.
- [3] R. Esmaeli, H. Aliniagerdroudbari, A. Nazari et al., "Optimization of a rainbow piezoelectric energy harvesting system for tire monitoring applications," in *Proceedings of ASME 2018 12th International Conference on Energy Sustainability*, Lake Buena Vista, FL, USA, June 2018.
- [4] C. Giles, B. Sabey, and K. Cardew, "Development and performance of the portable skid-resistance tester," in *Proceedings of Symposium on Skid Resistance*, ASTM International, New York, NY, USA, June 1962.
- [5] U. S. N. T. S. Board, *Fatal Highway Accidents on Wet Pavement-Magnitude, Location, and Characteristics*, National Transportation Safety Board, Washington, DC, USA, 1980.
- [6] H. Brodsky and A. S. Hakkert, "Risk of a road accident in rainy weather," *Accident Analysis & Prevention*, vol. 20, no. 3, pp. 161–176, 1988.
- [7] W. E. Meyer, *Frictional Interaction of Tire and Pavement (No. 793)*, ASTM International, West Conshohocken, PA, USA, 1983.
- [8] J. S. Kuttesch, "Quantifying the relationship between skid resistance and wet weather accidents for Virginia data," M.S. thesis, Virginia Polytechnic Institute and State University, Blacksburg, VA, USA, 2004.
- [9] R. Bond, G. F. Morton, and L. H. Krol, "A tailor-made polymer for tyre applications," *Polymer*, vol. 25, no. 1, pp. 132–140, 1984.
- [10] R. R. Rahalkar, "Dependence of wet skid resistance upon the entanglement density and chain mobility according to the Rouse theory of viscoelasticity," *Rubber Chemistry and Technology*, vol. 62, no. 2, pp. 246–271, 1989.
- [11] C. M. Roland, "Mechanical behavior of rubber at high strain rates," *Rubber Chemistry and Technology*, vol. 79, no. 3, pp. 429–459, 2006.
- [12] C. M. Roland, "Relaxation phenomena in vitrifying polymers and molecular liquids," *Macromolecules*, vol. 43, no. 19, pp. 7875–7890, 2010.
- [13] M. L. Miller, *The Structure of Polymers*, Van Nostrand Reinhold Inc., New York, NY, USA, 1966.
- [14] T. Murayama, *Dynamic Mechanical Analysis of Polymeric Material*, Elsevier Scientific Publishing Co., Amsterdam, Netherlands, 1978.
- [15] J. D. Ferry, *Viscoelastic Properties of Polymers*, John Wiley & Sons, Hoboken, NJ, USA, 1980.

- [16] N. McCrum, B. Read, and G. Williams, *Anelastic and Dielectric Properties of Polymeric Solids*, John Wiley & Sons, Chichester, UK, 1967.
- [17] K. P. Menard, *Dynamic Mechanical Analysis: A Practical Introduction*, CRC Press, Boca Raton, FL, USA, 2008.
- [18] M. A. Kashfipour, N. Mehra, and J. Zhu, "A review on the role of interface in mechanical, thermal, and electrical properties of polymer composites," *Advanced Composites and Hybrid Materials*, vol. 1, no. 3, pp. 415–439, 2018.
- [19] A. W. Nolle, "Methods for measuring dynamic mechanical properties of rubber-like materials," *Journal of Applied Physics*, vol. 19, no. 8, pp. 753–774, 1948.
- [20] K. te Nijenhuis, "Survey of measuring techniques for the determination of the dynamic moduli," in *Rheology*, pp. 263–282, Springer, Berlin, Germany, 1980.
- [21] ASTM, American Standards and Test Methods, 2017, <http://www.astm.org/>.
- [22] M. L. Williams, R. F. Landel, and J. D. Ferry, "The temperature dependence of relaxation mechanisms in amorphous polymers and other glass-forming liquids," *Journal of the American Chemical Society*, vol. 77, no. 14, pp. 3701–3707, 1955.
- [23] G. Hamed, "Free volume theory and the WLF equation," *Elastomerics*, vol. 120, pp. 14–17, 1988.
- [24] S. Sihn and S. W. Tsai, "Automated shift for time-temperature superposition," in *Proceedings of the 12th International Committee on Composite Materials*, vol. 51, p. 47, Paris, France, July 1999.
- [25] M. Harrison, A. O. Sykes, and M. Martin, "Wave effects in isolation mounts," *Journal of the Acoustical Society of America*, vol. 24, no. 1, pp. 62–71, 1952.
- [26] R. G. DeJong, G. E. Ermer, C. S. Paydenkar, and T. M. Remtema, "High frequency dynamic properties of rubber isolation elements," in *National Conference on Noise Control Engineering*, vol. 16, pp. 383–390, Noise Control Foundation, Ypsilanti, MI, USA, 1998.
- [27] N. Vahdati and L. K. L. Saunders, "High frequency testing of rubber mounts," *ISA Transactions*, vol. 41, no. 2, pp. 145–154, 2002.
- [28] G. Ramorino, D. Vetturi, D. Cambiaghi, A. Pegoretti, and T. Ricco, "Developments in dynamic testing of rubber compounds: assessment of non-linear effects," *Polymer Testing*, vol. 22, no. 6, pp. 681–687, 2003.
- [29] M. J. Grudd, "Value of variable sources on power systems," *IEE Proceedings C Generation, Transmission and Distribution*, vol. 138, no. 2, pp. 149–165, 1991.
- [30] H. Mouri and K. Akutagawa, "Improved tire wet traction through the use of mineral fillers," *Rubber Chemistry and Technology*, vol. 72, no. 5, pp. 960–968, 1999.
- [31] O. Kramer and J. D. Ferry, "Dynamic mechanical properties," *Science and Technology of Rubber*, pp. 179–221, 1978.
- [32] P. M. Sheridan, F. O. James, and T. S. Miller, "Design of components," in *Engineering with Rubber*, pp. 209–235, Hanser, Munich, Germany, 1992.
- [33] A. N. Gent, *Engineering with Rubber: How to Design Rubber Components*, Carl Hanser Verlag GmbH Co KG, Munich, Germany, 2012.
- [34] T. Benson, *Shape Effects on Drag*, NASA Webpage, Washington, DC, USA, June 2017, <https://www.grc.nasa.gov/www/k-12/rocket/shaped.html>.
- [35] R. Esmaeeli, A. Nazari, H. Aliniagerdroudbar et al., "Heat built up during dynamic mechanical analysis (DMA) testing of rubber specimens," in *Proceedings of Volume 9: Mechanics of Solids, Structures, and Fluids*, no. 52149, p. V009T12A059, Pittsburgh, PA, USA, November 2018.
- [36] J. Griffin, D. Martin, and R. Siron, "Quadruple lap simple shear test specimen," Google Patents, 1973.
- [37] ASTM D5992-96(2018), Standard Guide for Dynamic Testing of Vulcanized Rubber and Rubber-Like Materials Using Vibratory Methods, ASTM International, West Conshohocken, PA, USA, 2018, <http://www.astm.org>.
- [38] S. Farhad and R. Esmaeeli, "Dynamic mechanical analysis system," Google Patents Application Number: 20190017912, 2019.